Review Article

# Progress of Hard X-ray Photoemission Spectroscopy in a Decade; Its Bulk Sensitivity, Recoil Effects, and Polarization Dependence

Photoemission spectroscopy in the hard X-ray region has been one of the most improved experimental techniques since the development of insertion devices in the third-generation high-brilliance synchrotron radiation facilities, and has overcome the drawbacks of conventional photoemission for probing bulk electronic states such as surface sensitivity in the case of low-energy excitation (<~1 keV), as schematically shown in Fig. 1, and insufficiently low throughput in the case of high-energy excitation. Practical hard X-ray photoemission, known as HAXPES, has been established at undulator beamlines since 2000 [1,2], especially at SPring-8. As originally expected, HAXPES is employed for investigating the bulk and/or varied interface electronic structures of functional materials. On the other hand, a few intrinsic features of HAXPES have been revealed for this decade in addition to its bulk sensitivity. Here several HAXPES studies using these features are reviewed.

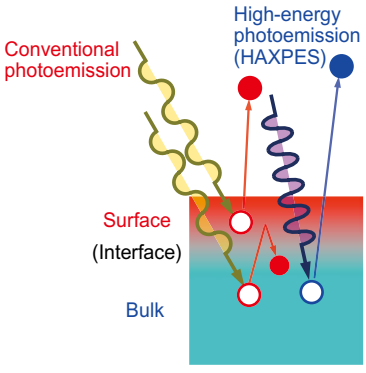


Fig. 1. Schematic diagram showing bulk sensitivity of HAXPES compared with that of conventional photoemission spectroscopy.

## 1. Instrumentation of HAXPES at BL19LXU

There are several setups for utilizing HAXPES at SPring-8. The setup of the beamline optics for HAXPES at BL19LXU is displayed in Fig. 2. The relative energy resolution of the beams supplied by the standard double-crystal Si(111) monochromator of typical hard X-ray beamlines in SPring-8, $\Delta E/E \sim 10^{-4}$, is insufficient for HAXPES at photon energies of several keV. Thus, a post-monochromator called a channel-cut crystal is usually employed. A Si(111) channel-cut crystal is often used in several beamlines in SPring-8 to obtain high energy resolution since the discrete photon energies can be selected from $h\nu \cong 6$, 8, and 10 keV using the (333), (444), and (555) reflections, where $\Delta E \sim 60$, 40, and 20 meV are available at $h\nu \cong 6$, 8, and 10 keV, respectively, without changing the beam path. To obtain higher photon flux, another Si channel-cut crystal with lower indices such as (311), (331), and (620) is used. The Si(620) reflection gives $\Delta E \sim 50$ meV at $h\nu = 7.9$ keV in BL19LXU. An overall experimental resolution of ~65 meV has so far been achieved [3]. Typical overall resolutions are set to 250–500 meV, which are sufficient for core-level photoemission in most cases since the lifetime broadening is similar to or larger than the above values.

The beam originally supplied from the undulator is horizontally linearly polarized. In the hard X-ray region with $h\nu = 5$–16 keV, a single-crystalline diamond is used as a phase retarder to switch the polarization, but the use of double single-crystalline diamonds, which compensate for the phase-shift inhomogeneity due to the angular divergence of the incoming X-ray beam, gives better polarization with a degree of linear polarization $P_L$ close to ±1. As shown in Fig. 2, (100) diamonds are employed in BL19LXU, giving the (220) Bragg reflection with Laue geometry at $h\nu$ ~8 keV [4]. The horizontally polarized photons from the undulator are transformed into circular polarization by the first diamond plate, and a vertically polarized

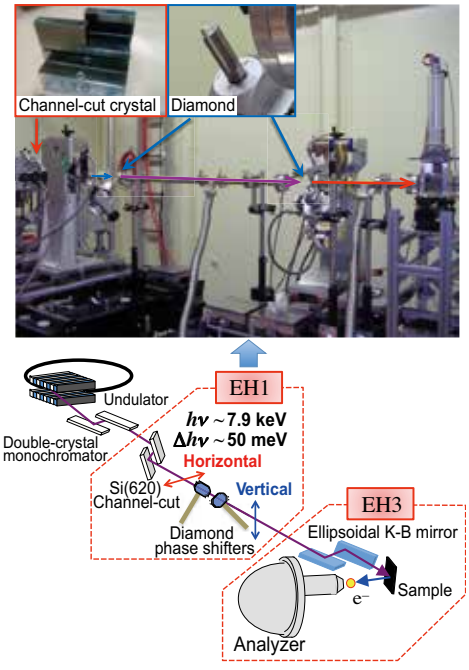


Fig. 2. Beamline optics for (polarized) HAXPES, Si channel-cut crystal, and single-crystalline diamond phase retarder.

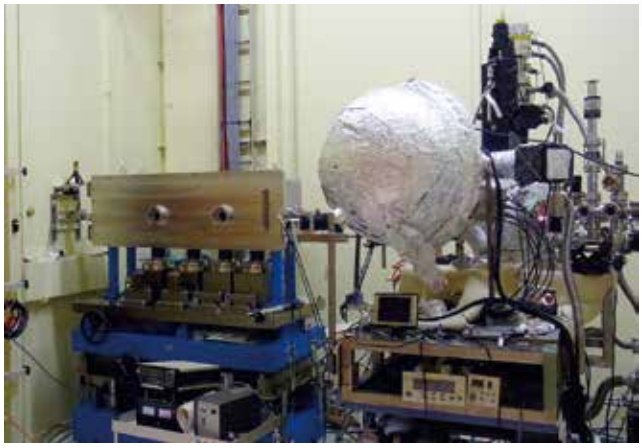

Fig. 3. Photograph of the hemispherical photoelectron spectrometer and focusing mirror for HAXPES.

X-ray is obtained by setting the optimized offset angle for the second plate. Vertical polarization with $P_L$ better than –0.9 has been achieved at BL19LXU, which corresponds to over 95% of the components being vertically polarized. The thickness of each diamond is 0.25 mm and the transmittance of the X-ray beam after the double-crystal phase shifter is ~50%. Subsequently, the X-ray beam is focused onto the sample in the spectrometer chamber using an ellipsoidal Kirkpatrick-Baez mirror as shown in Fig. 3, where a focused spot size of ~25 μm × ~25 μm is feasible for HAXPES. In our HAXPES measurements, a lens mode with a magnification of 12, which is larger than that (= 5) for conventional angle-integrated soft X-ray and VUV photoemission, is employed.

## 2. Bulk electronic structures probed by HAXPES

In strongly correlated electron systems in which the on-site Coulomb repulsion $U$ is not negligible, the electronic structure is often determined as a function of $U/W$, where $W$ denotes the width of the bare band formed by the strongly correlated orbitals. Since $W$ is reduced at the surface, the electronic states are often substantially different between the bulk and surface. When conventional photoemission with $h\nu < 1.5$ keV is applied to the core-level photoemission of strongly correlated electron systems, the contributions of the surface to the spectra prevent the clarifying of the bulk electronic states. Figure 4 shows a comparison between the $Yb^{2+}$ $4f$ photoemission spectra near $E_F$ at $h\nu = 700$ and 8180 eV for the Kondo semiconductor $YbB_{12}$ [3,5]. There is a peak structure due to the $Yb^{2+}$ $4f_{7/2}$ state in the vicinity of the Fermi level ($E_F$) in both spectra. In addition, one can observe the $4f$ contributions of the surface $Yb^{2+}$ at the binding energy of ~0.9 eV in the spectrum at $h\nu$ = 700 eV with an energy resolution of ~100 meV, while such a surface contribution is negligible in the spectrum at $h\nu$ = 8180 eV with an energy resolution of ~65 meV.

Another example of HAXPES for strongly correlated materials is shown in Fig. 5, which shows valence-band photoemission spectra of the paradigmatic Mott transition system $V_2O_3$ [6]. As displayed in the figure, there is a prominent quasi-particle peak just below $E_F$ and a small bump structure around –1.3 eV ascribed to the so-called lower Hubbard band (LHB) in the paramagnetic metallic (PM) phase. The relative weight of the quasi-particle peak is greater at $h\nu = 8180$ eV than at $h\nu = 700$ eV, which reflects the enhancement of the bulk contribution at $h\nu$ = 8180 eV due to the longer probing depth. The "bulk" photoemission spectrum extracted from the low-energy excitation data is in excellent agreement with the HAXPES spectrum, which indicates that HAXPES with $h\nu$ ~8 keV is truly bulk sensitive. On the other hand, the spectral weight is negligible in the antiferromagnetic insulating (AFI) phase, showing a gap opening. In addition, two spectral components are observed between $E_F$ and –3 eV in the HAXPES spectrum in the AFI phase. One is a peak centered at –0.5 eV and the other is a shoulder at –1.3 eV close to the energy of the LHB in the PM phase. The spectral shape has $h\nu$ dependence, where the intensity of the former peak relatively increases with $h\nu$. The bulk spectrum extracted from the spectra at $h\nu = 700$ and 220 eV well reproduces the HAXPES spectrum, as seen in the PM phase. The shoulder centered at –1.3 eV has been concluded as LHB, which suggests that $U$ is unchanged across the transitions and that the so-called orbital-selective Mott transition scenario is the most plausible for $V_2O_3$.

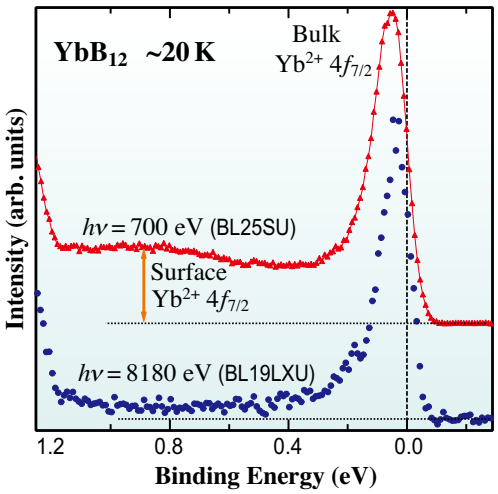


Fig. 4. Comparison of the HAXPES spectrum of $YbB_{12}$ near $E_F$ at $h\nu$ = 8180 eV with the soft X-ray photoemission spectrum at $h\nu$ = 700 eV. The spectrum at 700 eV was obtained at BL25SU.

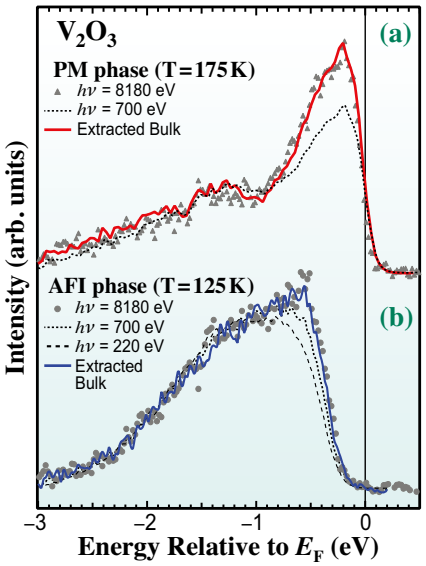


Fig. 5. Photon energy dependence of the valence-band photoemission spectra of $V_2O_3$ near $E_F$ in the metallic and insulating phases as well as the "extracted" bulk spectra obtained from low-energy photoemission.

## 3. Recoil effects

For photoemission in solids, the basic formula $E_B = h\nu - E_K\phi$ applies, where $E_B$, $E_K$, and $\phi$ denote the electron binding energy, photoelectron kinetic energy, and the work function of the solid, respectively. In the photoemission from a single free atom with mass $M$, however, the recoil energy $E_R \cong (m/M)E_K$ is given to the photoionized atom, where $m$ is the electron mass. The resulting $E_K$ is thus slightly decreased by the amount $E_R$. While this recoil effect has been observed in the photoemission spectra of core levels in gases [7], it has been verified in solids [8,9] by the combination of HAXPES and soft X-ray photoemission with a lower $h\nu$ than that for HAXPES. A characteristic of the recoil effects is that $E_R$ is larger for light elements. Figure 6 shows the hard and soft X-ray B 1*s* and Yb 4*d* core-level spectra of $Yb_{7/8}Lu_{1/8}B_{12}$ [9]. Although the shift of the peak binding energy with the change in the excitation energy is negligible for the Yb 4*d* spectra, it is noticeable and as large as ~300 meV for the B 1*s* spectra, which is comparable to $E_R$ of ~400 meV. This difference between the light and heavy elements undoubtedly reflects the recoil effects in solids. Rather surprisingly, the recoil effects are not restricted to core-level excitations and are also seen in valence-band excitations, which has been verified by the $h\nu$ dependence of the valence-band photoemission for metallic Al, where the Fermi cutoff is shifted towards a higher $E_B$ [10,11] as if an energy gap were opened in the HAXPES spectra. These phenomena suggest that the photoemission process takes place in the vicinity of the nucleus even for nearly free electrons in solids. On the other hand, the recoil effects are absent in the spectra near $E_F$ for bulk $VO_2$ [12], which are correlated to the Debye temperature of materials.

## 4. Polarization dependence

In addition to bulk sensitivity, HAXPES at $h\nu$ = 5–10 keV has the unique characteristics of having photoionization cross sections for the *s* and *p* states comparable to those for the *d* and *f* states as well as strong orbital dependence of the photoelectron angular distribution with respect to the light polarization. As an overall tendency, the photoelectron intensity for the *s* state is strongly suppressed in the *s*-polarization configuration (*s*-pol., see the inset of Fig. 7) compared with the *p*-polarization configuration (*p*-pol.), while the *d* and *f* spectral weights are not significantly suppressed even in *s*-pol. Therefore, the extraction of the *s* contributions as well as the *d* and *f* contributions in the bulk valence band of solids becomes feasible by linear-polarization-dependent HAXPES. Figure 7 shows the polarization dependence of the valence-band HAXPES spectrum for polycrystalline silver. It can be seen that the spectral weight from $E_F$ to 3 eV is relatively reduced in *s*-pol. This behavior indicates that the 4*d* bands are located far below $E_F$ and are well separated from the conduction 5*sp* band crossing $E_F$ for silver. In contrast, it has been

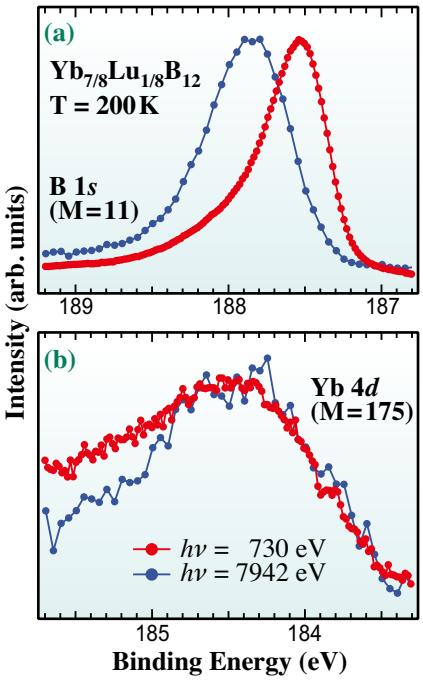


Fig. 6. Photon energy dependence of the B 1*s* and Yb 4*d* core-level photoemission spectra of $Yb_{7/8}Lu_{1/8}B_{12}$ demonstrating the recoil effects in the photoemission process of crystalline solids. M indicates mass of the atoms.

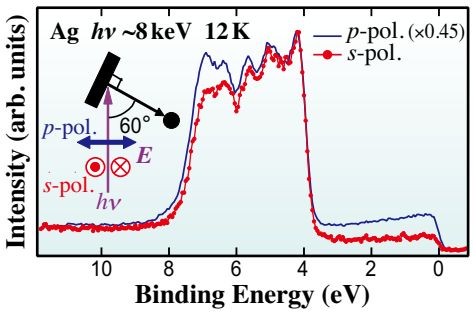


Fig. 7. Linear-polarization-dependent valence-band HAXPES spectra of polycrystalline silver. The inset shows the experimental geometry of the HAXPES measurements.

found that the 5*d* contributions to the conduction electrons are prominent in gold by polarization-dependent HAXPES [13].

Polarization dependence (linear dichroism (LD) in other words) is also seen in the *angle-resolved* core-level photoemission spectra (in other words, angular distributions of photoelectrons excited from core levels determined by the selection rules) of a partially filled subshell with a so-called multiplet structure for single-crystalline materials. (Note that an acceptance angle of ±several degrees is sufficient in this angle-resolved measurements.) Since the LD in the multiplet structure reflects the anisotropy in the Coulomb and exchange interactions between the electrons in a single site, the anisotropic charge distributions of a strongly correlated orbital with localized character can be revealed by LD in angle-resolved core-level HAXPES. The LD in angle-resolved $Yb^{3+}$ $3d_{5/2}$ core-level HAXPES spectra was first observed for tetragonal $YbCu_2Si_2$ and $YbRh_2Si_2$, reflecting the 4*f*-orbital symmetry in the ground and excited states [14]. Here it should be emphasized that the LD was also seen even in a rather highly symmetric cubic crystal structure. Indeed, the $\Gamma_8$ ground-state symmetry for cubic $YbB_{12}$ has been verified by the LD in the $Yb^{3+}$ $3d_{5/2}$ core-level photoemission along the [100] and [111] directions, where the LD is mutually flipped at the same $E_B$ [15]. These phenomena are not restricted to the Yb compounds and are widely seen in many rare-earth elements as shown in Fig. 8, which displays the polarization dependence of the $Sm^{3+}$ $3d_{5/2}$ core-level HAXPES spectrum [16]. There is a main peak at a binding energy of 1081 eV and a shoulder structure at 1083 eV in the spectra, which correspond to the $Sm^{3+}$ $3d^9 4f^5$ multiplet structure. The LD in the $Sm^{3+}$ $3d_{5/2}$ spectra was clearly observed, where the peak at 1081 eV is stronger in *p*-pol. than in *s*-pol. but the spectral weight of the shoulder at 1083 eV is stronger in *s*-pol., which reflects the deviation of the anisotropic $Sm^{3+}$ 4*f* distribution from the spherical symmetry.

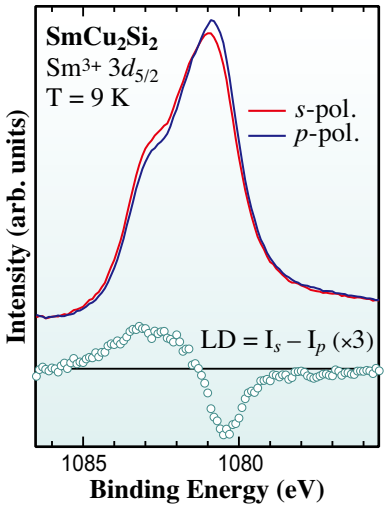


Fig. 8. Polarization dependence of the *angle-resolved* $Sm^{3+}$ $3d_{5/2}$ core-level HAXPES spectrum along the [001] direction and the linear dichroism for $SmCu_2Si_2$.

## 5. Summary

Several HAXPES studies utilizing the characteristic features of HAXPES were reviewed. Although HAXPES studies such as those with momentum resolution and/or standing wave [17] and depth analysis [18] were not introduced here, the unique potential of HAXPES for investigating strongly correlated systems, functional materials, and buried interfaces will lead to many valuable clarifications of electronic structures.

Akira Sekiyama[a,b]

[a] Division of Materials Physics, Osaka University
[b] RIKEN SPring-8 Center

Email: sekiyama@mp.es.osaka-u.ac.jp

**References**

[1] K. Kobayashi *et al.*: Appl. Phys. Lett. **83** (2003) 1005.
[2] S. Thiess *et al.*: Solid State Commun. **132** (2004) 589.
[3] A. Sekiyama: J. Electron Spectrosc. Relat. Phenom. **208** (2016) 100.
[4] H. Fujiwara *et al.*: J. Synchrotron Rad. **23** (2016) 735.
[5] J. Yamaguchi *et al.*: Phys. Rev. B **79** (2009) 125121.
[6] H. Fujiwara *et al.*: Phys. Rev. B **84** (2011) 075117.
[7] L. Åsbrink: Chem. Phys. Lett. **7** (1970) 549.
[8] Y. Takata *et al.*: Phys. Rev. B **75** (2007) 233404.
[9] S. Suga and A. Sekiyama: Eur. Phys. J. Spec. Topic **169** (2009) 227.
[10] Y. Takata *et al.*: Phys. Rev. Lett. **101** (2008) 137601.
[11] S. Suga and A. Sekiyama: J. Electron Spectrosc. Relat. Phenom. **181** (2010) 48.
[12] S. Suga *et al.*: New J. Phys. **11** (2009) 073025.
[13] A. Sekiyama *et al.*: New J. Phys. **12** (2010) 043045.
[14] T. Mori *et al.*: J. Phys. Soc. Jpn. **83** (2014) 123702.
[15] Y. Kanai *et al.*: J. Phys. Soc. Jpn. **84** (2015) 073705.
[16] Y. Kanai *et al.*: J. Electron Spectrosc. Relat. Phenom. (2017) - in press.
[17] C.S. Fadely: J. Electron Spectrosc. Relat. Phenom. **190** (2013) 165.
[18] E. Ikenaga *et al.*: J. Electron Spectrosc. Relat. Phenom. **190** (2013) 180.